Gut Pathogens

RESEARCH Open Access

Species-level dynamics of gastric microbiome after *Helicobacter pylori* eradication in high-risk Mongolian population

Namsrai Renchinsengee[1,3], Saruuljavkhlan Batsaikhan[1,2,3], Ayush Khangai[1], Gantuya Boldbaatar[2,3], Bayasgalan Luvsandagva[4], Aigul Lazatkhan[6], Davaadorj Duger[2,3], Oyuntsetseg Khasag[3], Takashi Matsumoto[1,5] and Yoshio Yamaoka[1,5,7*]

Abstract

Background Species-level resolution is essential to understand gastric microbiome recovery after *Helicobacter pylori* eradication, yet short-read 16 S rRNA approaches often obscure clinically relevant changes.

Methods Gastric biopsies from 121 adults in Bayan-Ölgii, Mongolia (71 *H. pylori*–positive, 50 *H. pylori*–negative) were analyzed, including nine paired pre- and post-eradication gastric biopsy samples collected six months apart, enabling exploratory longitudinal analysis. Full-length 16 S rRNA (V1–V9) sequencing was performed using the Oxford Nanopore platform with EMU taxonomic assignment (SILVA v138.1/NCBI RefSeq). Ecological changes were evaluated using diversity indices, principal coordinates analysis (PCoA) with PERMANOVA, and differential abundance testing (DESeq2, FDR < 0.05). Eradication therapy (esomeprazole–bismuth–doxycycline–levofloxacin) achieved success in 54 of 57 *H. pylori*–positive patients (94.7%).

Results *H. pylori*–positive microbiomes were dominated by *H. pylori* (91.8% ± 3.9%) and exhibited markedly reduced diversity (Shannon = 0.44 ± 0.11) compared with *H. pylori*–negative samples (2.08 ± 0.25; $p < 0.001$). Six months after eradication, diversity increased significantly (2.17 ± 0.20; $p = 0.0001$), with enrichment of oral commensals including *Streptococcus mitis* (↑ 11.9×), *Neisseria elongata* (↑ 13.7×), and *Prevotella melaninogenica* (↑ 13.0×). However, post-eradication profiles at six months remained distinct from *H. pylori*–negative communities (PERMANOVA $R^2 = 0.12$; $p = 0.02$). In total, 174 amplicon sequence variants changed significantly, including persistence of *Fusobacterium nucleatum*.

Conclusions Nanopore full-length 16 S sequencing reveals fine-scale, clinically relevant shifts that are masked by partial-gene assays. Eradication rapidly restores microbial diversity, but at six months, is associated with a novel ecological equilibrium rather than complete normalization. This species-resolved approach offers a practical framework for post-eradication microbiome monitoring and may inform strategies to reduce residual gastric cancer risk in high-burden populations.

*Correspondence:
Yoshio Yamaoka
yyamaoka@oita-u.ac.jp

Full list of author information is available at the end of the article

Introduction

Helicobacter pylori is a gram-negative, microaerophilic bacterium that persistently colonizes the human stomach and is the principal cause of chronic gastritis, peptic ulcer disease, and gastric cancer (GC) [1–3]. GC is the fifth most common malignancy and the third leading cause of cancer-related mortality worldwide [4]. Mongolia carries the highest global burden, with an age-standardized incidence rate of 35.5 per 100,000 and a mortality rate of 31.6 per 100,000, figures that are closely linked to the country's exceptionally high prevalence of *H. pylori* infection [5–7]. In addition, genomic analyses of Mongolian *H. pylori* strains show distinct virulence gene patterns and subgroups linked to carcinogenesis [8].

The stomach is now recognized to harbor a diverse microbial community that plays essential roles in mucosal immunity, inflammation, and carcinogenesis [9, 10]. Chronic *H. pylori* infection markedly reduces microbial diversity and alters community structure [11–13], but the extent and pace of recovery following eradication—particularly at the species level—remain incompletely defined [14, 15]. Recent longitudinal studies have shown that although *H. pylori* eradication increases gastric microbial diversity, the post-eradication community does not fully revert to that of uninfected individuals [16]. Instead, oral-associated taxa and non-*H. pylori* bacteria often become enriched, a shift linked to persistent inflammation and residual risk of GC progression. The broader ecological consequences of eradication on the gastric microbiome therefore remain poorly understood, especially in high-risk populations [7, 17].

Most post-eradication studies to date have been conducted in Western or East Asian populations using short-read 16 S rRNA sequencing, which typically targets only partial regions (e.g., V3–V4). This approach limits taxonomic resolution and often obscures species-level shifts that may be critical for understanding gastric carcinogenesis [17, 18]. In contrast, full-length V1–V9 16 S rRNA profiling with Oxford Nanopore sequencing captures the entire gene, enabling more accurate species-level classification and detection of subtle community changes [19, 20]. Mongolia provides a unique model for such investigations due to its distinct dietary patterns, host genetic background, and exceptionally high risk of gastric cancer [3, 6, 7]. Recent genomic work in the isolates from Mongolia further supports heightened oncogenic potential tied to strain background [8]. Defining post-eradication microbial restructuring in this context may reveal mechanisms of mucosal healing, identify biomarkers predictive of long-term cancer risk, and inform microbiome-targeted interventions such as probiotics or dietary modification [21, 22].

Here, we applied full-length 16 S rRNA sequencing on the Oxford Nanopore MinION platform to achieve species-level resolution of the gastric microbiome. We analyzed paired gastric biopsies from Mongolian dyspeptic patients before and six months after successful *H. pylori* eradication, together with *H. pylori*–negative controls. Our objectives were to (i) characterize baseline microbial differences at the species level, (ii) assess diversity recovery following eradication, and (iii) identify key taxa driving community reassembly. To our knowledge, this is the first high-resolution, longitudinal analysis of the gastric microbiome in a high-risk Mongolian population, providing insights critical for reducing long-term gastric cancer risk after *H. pylori* eradication.

Materials and methods

Study population and sample collection

We enrolled 121 adult Mongolian patients with dyspeptic symptoms at Bayan-Ölgii Provincial Hospital. Participants ranged in age from 29 to 74 years (mean ± SD, 51.8 ± 11.0 years) and included 62 females (51.2%) and 59 males (48.8%). None had received prior *H. pylori* eradication therapy. Exclusion criteria were: (i) history of gastric surgery; (ii) use of antibiotics, bismuth compounds, or proton-pump inhibitors within the preceding 4 weeks; and (iii) significant systemic illness, including chronic liver, renal, or autoimmune disease.

All participants underwent diagnostic upper gastrointestinal endoscopy. From each subject, paired gastric biopsies were obtained from the antrum and corpus. For each site, one biopsy was placed in transport medium and another in RNAlater (Thermo Fisher Scientific, USA), resulting in two vials per medium type. Additional specimens were fixed in 10% neutral buffered formalin for histological and immunohistochemical assessment of gastritis, atrophy, and intestinal metaplasia. A separate antral biopsy was immediately inoculated into the rapid urease test (RUT) medium to evaluate *Helicobacter pylori* urease activity. Biopsies preserved in RNAlater were stored at − 80 °C until DNA extraction, whereas those in transport medium were processed for *H. pylori* culture under microaerophilic conditions. This multi-sample allocation strategy was based on the Updated Sydney System, with minor modifications to accommodate microbiome sequencing requirements [23].

H. pylori infection detection

At enrollment, *H. pylori* status was determined using a combination of RUT and histology with IHC on antral biopsies. RUT was performed immediately after endoscopy according to the manufacturer's instructions [24]. Histological evaluation included hematoxylin–eosin staining for gastritis grading and detection of curved bacilli, while IHC with a monoclonal anti-*H. pylori* antibody was applied to enhance diagnostic sensitivity and specificity [25]. Patients were classified as

H. pylori–positive if either RUT or histology/IHC was positive, and as *H. pylori*–negative only if all tests were negative.

All RUT-positive patients were offered eradication therapy. Eradication success was confirmed by stool antigen testing at 2 months; in patients undergoing repeat endoscopy, biopsy-based RUT was also performed at 6 months.

Histological evaluation

Biopsies were obtained from the greater curvature of the antrum (≈ 2 cm proximal to the pylorus) and the corpus (8–10 cm distal to the gastroesophageal junction). Samples were fixed in 10% neutral-buffered formalin, paraffin-embedded, and stained with hematoxylin–eosin and May–Giemsa. Histological assessment was performed by an experienced gastrointestinal pathologist blinded to *H. pylori* status. Polymorphonuclear and mononuclear cell infiltration, glandular atrophy, and intestinal metaplasia (IM) were graded according to the Updated Sydney System [23], and atrophy was further staged using the Operative Link on Gastritis Assessment (OLGA) system [26]. Based on these criteria, participants were classified into four histological categories: normal mucosa, gastritis, atrophy, and IM.

H. pylori detection and eradication therapy

All RUT-positive patients were offered eradication therapy consisting of esomeprazole (40 mg once daily) and bismuth subsalicylate (524 mg twice daily) for 30 days, combined with doxycycline (100 mg twice daily) and levofloxacin (500 mg once daily) for 14 days.

This modified bismuth quadruple regimen was used as the *first-line therapy*, selected based on local antibiotic resistance data and consistent with international guideline recommendations for regions with high clarithromycin resistance [27]. Eradication success was confirmed by stool antigen testing at two months. Patients with persistent infection were advised to undergo further management, although second-line therapy was not included within the scope of this study. A longitudinal subset of nine successfully treated patients underwent repeat endoscopy with gastric biopsy six months after eradication for microbiome analysis.

DNA extraction and 16 S rRNA gene sequencing

Microbial DNA was extracted from RNAlater-preserved gastric biopsy specimens using the DNeasy Blood & Tissue Kit (Qiagen, Hilden, Germany) according to the manufacturer's instructions. DNA concentration was measured using a Qubit 4 Fluorometer with the Qubit dsDNA High Sensitivity Assay Kit (Thermo Fisher Scientific, USA), and samples were normalized prior to amplification.

The full-length bacterial 16 S rRNA gene (~ 1.5 kb) was amplified using universal primers 27 F (5′-AGAGTTTGATCMTGGCTCAG-3′) and 1492R (5′-GGTTACCTTGTTACGACTT-3′). Amplicons were prepared using Oxford Nanopore barcoded amplicon library reagents following the manufacturer's protocol for full-length 16 S rRNA sequencing (Oxford Nanopore Technologies, UK). Libraries were purified, quantified, pooled at equimolar concentrations, and loaded onto R9.4.1 flow cells (FLO-MIN106D).

Sequencing was performed on a GridION sequencing device, which enables parallel operation of multiple MinION flow cells, using MinKNOW v22.12.5. Runs were conducted for approximately 48 h, depending on sequencing yield. Basecalling was performed using Guppy v6.4.6 in high-accuracy (HAC) mode. Negative extraction controls and no-template PCR controls were included throughout library preparation and sequencing to monitor potential contamination.

Sequence processing and taxonomic assignment

Raw FASTQ reads were demultiplexed and adapter-trimmed with Porechop v0.2.4, then quality- and size-filtered using NanoFilt v2.8.0 (≥ 1 kb, Q ≥ 10) [20]. High-quality reads were processed with the EMU pipeline (v3.2.3, 2023 release) for amplicon sequence variant (ASV) inference and chimera removal [16, 20]. Taxonomic assignment was performed against the SILVA v138.1 (30) and NCBI RefSeq databases (Release 210, July 2023) [28, 29]. To ensure balanced sequencing depth across samples, the ASV table was rarefied to 10,000 reads per sample prior to analysis.

Microbiome analyses

Alpha diversity (Shannon and Simpson indices) and Bray–Curtis beta diversity were calculated using the Phyloseq package v1.42.0 [30]. Principal coordinates analysis (PCoA) was applied to visualize group separation, with significance assessed by PERMANOVA [31]. Differential abundance testing was performed in DESeq2 v1.38.0 [32] using Wald tests with Benjamini–Hochberg false discovery rate (FDR) correction [33], and taxa with FDR < 0.05 were considered significant. To explore ecological associations, the 10 most prevalent taxa were transformed using centered log-ratio with a pseudo-count of 1, and pairwise Spearman correlations were calculated. Correlations with $|\rho| > 0.55$ were retained to construct undirected networks in igraph v1.5.0 [34] and visualized with ggraph v4.3.1 (Table 1).

Results

A total of 121 adults with dyspepsia were enrolled and underwent upper gastrointestinal endoscopy at Bayan-Ölgii Provincial Hospital. The cohort had a mean age

Table 1 Demographic, endoscopic, and histological characteristics of the study population

(A) Baseline demographics of 121 participants stratified by *H. pylori* infection status showing no significant differences in age or sex distribution between groups

(B) Kyoto endoscopy scores comparing *H. pylori*–negative and *H. pylori*–positive individuals demonstrate significantly higher intestinal metaplasia, enlarged folds, nodularity, and total Kyoto scores in the *H. pylori*–positive group ($p < 0.05$)

(C) Paired analysis before and six months after eradication shows marked improvement in diffuse redness and total Kyoto scores ($p < 0.05$)

(D) Distribution of histological stages according to OLGA and OLGIM systems

(E) Histological grading of *H. pylori* density, inflammatory cell infiltration, atrophy, and intestinal metaplasia in antrum, angle, and corpus before and six months after eradication therapy. Data are presented as mean ± SD (0 = none, 1 = mild, 2 = moderate, 3 = severe). *p* values were calculated using the Wilcoxon signed-rank test for paired samples ($n = 9$)

Table 2 A. Baseline demographics by *H. pylori* status

Group (diagnostic)	*N*	Age (mean ± SD)	Sex, *n* (%) per group
HP– (negative)	50	48.3 ± 10.9	Female: 29 (58.0%) | Male: 21 (42.0%)
HP+ (positive)	71	52.2 ± 11.2	Female: 33 (46.5%) | Male: 38 (53.5%)
Total baseline	121	51.8 ± 11.0	Female: 62 (51.2%) | Male: 59 (48.8%)

Table 3 B. Kyoto endoscopy scores at baseline by *H. pylori* status

Feature	HP– (mean ± SD)	HP+ (mean ± SD)	All participants (mean ± SD)	*p* value	sig
Atrophy	1.22 ± 0.47	1.39 ± 0.64	1.32 ± 0.58	0.1157	ns
Intestinal metaplasia	0.82 ± 0.65	1.11 ± 0.84	0.98 ± 0.78	0.0457	*
Diffuse redness	1.09 ± 0.67	1.25 ± 0.75	1.17 ± 0.72	0.2577	ns
Enlarged folds	0.20 ± 0.40	0.41 ± 0.50	0.32 ± 0.47	0.0184	*
Nodularity	0.09 ± 0.29	0.23 ± 0.42	0.17 ± 0.38	0.0447	*
Total	3.42 ± 1.51	4.39 ± 2.31	3.96 ± 2.07	0.0104	*

of 51.8 ± 11.0 years (range, 29–74) and consisted of 62 females (51.2%) and 59 males (48.8%) (Table 2). Based on combined rapid urease testing and histology, 71 patients (58.7%) were classified as *H. pylori*–positive (HP+) and 50 (41.3%) as *H. pylori*–negative (HP–). The mean age was 52.2 ± 11.2 years among HP+ individuals and 48.3 ± 10.9 years among HP– individuals, indicating that infection tended to occur in slightly older patients. Sex distribution was balanced across groups, with females comprising 46.5% (33/71) of the HP+ group and 58.0% (29/50) of the HP– group.

Table 4 C. Paired Kyoto endoscopy scores before and 6 months after *H. pylori* eradication

Feature	Pre-treatment (mean ± SD)	6 mo Post-treatment (mean ± SD)	*p* value (paired)	sig
Atrophy	1.56 ± 0.53	1.56 ± 0.53	1.00	ns
Intestinal metaplasia	1.57 ± 0.53	1.22 ± 0.83	1.00	ns
Diffuse redness	1.33 ± 0.71	0.00 ± 0.00	0.0080	**
Enlarged folds	1.00 ± 0.00	0.00 ± 0.00	0.0625	ns
Nodularity	1.00 ± 0.00	0.22 ± 0.44	1.00	ns
Total	4.80 ± 2.52	3.00 ± 1.58	0.0083	**

Endoscopic findings based on the Kyoto classification of HP + and HP– participants

Endoscopic evaluation according to the Kyoto classification of gastritis revealed marked differences between the HP + and HP– groups [35]. Most HP+ patients exhibited moderate-to-severe atrophic changes, with intestinal metaplasia (IM) detected in 78.3% of cases, underscoring the advanced mucosal remodeling associated with chronic infection [6, 7, 23]. Quantitatively, the total Kyoto gastritis score was significantly higher in HP+ than HP– individuals (4.39 ± 2.31 vs. 3.42 ± 1.51; $p = 0.01$), confirming the stronger endoscopic evidence of gastritis among infected patients (Table 3). Among individual Kyoto components, intestinal metaplasia ($p = 0.045$), enlarged folds ($p = 0.018$), and nodularity ($p = 0.044$) were all significantly more frequent in the HP+ group, reflecting the chronic mucosal injury and regenerative changes characteristic of *H. pylori* infection. By contrast, diffuse redness did not differ significantly between groups ($p > 0.05$), indicating that this feature alone was not a specific marker of infection. In terms of severity, atrophy among HP+ patients was graded as mild in 31.0%, moderate in 45.1%, and severe in 23.9%, whereas HP– patients predominantly exhibited mild or absent atrophy ($p = 0.01$). Similarly, intestinal metaplasia was mild in 38.0%, moderate in 29.6%, and severe in 10.7% of HP+ cases, while nearly absent among HP– controls ($p < 0.001$) (Table 3). These data demonstrate that both the extent and severity of mucosal transformation were markedly greater in infected individuals, reflecting cumulative inflammatory damage. Active gastritis, characterized endoscopically by diffuse redness, mucosal swelling, and friability, predominated among HP+ patients, while inactive gastritis or normal mucosa predominated in HP– controls. Representative endoscopic views (Table 3) illustrate the antral nodularity and enlarged folds typical of active *H. pylori* infection compared with the smooth, pale mucosa of uninfected subjects (Table 4).

Correlation between endoscopic and histological findings in HP + and HP– participants

Endoscopic observations correlated closely with histological grading. Patients with higher Kyoto scores tended to exhibit corresponding histological severity, with OLGA and OLGIM stages ≥ II observed mainly among those with moderate-to-severe endoscopic atrophy or IM ($p < 0.01$) [35]. In contrast, HP– individuals with low Kyoto scores usually showed Stage 0–I changes, indicating minimal glandular loss or metaplasia. This concordance between endoscopic and histological staging underscores the reliability of the Kyoto classification in reflecting underlying mucosal pathology in this Mongolian cohort (Table 5).

Additional endoscopic observations

Other upper gastrointestinal findings highlighted the clinical heterogeneity of this dyspeptic population. Gastroesophageal reflux disease (GERD) was noted in a subset of patients—predominantly among HP– individuals—while bile reflux was occasionally observed in both groups. A few patients exhibited superficial Candida colonization, likely secondary to acid suppression or altered mucosal environments. Together, these findings emphasize the complex interplay between host factors, microbial colonization, and environmental exposures in shaping gastric mucosal health.

Microbial diversity based on the species level of HP + and HP– participants

Of the 71 HP+ patients enrolled in this study, 57 completed the prescribed quadruple therapy regimen, and eradication was successfully confirmed in 54 individuals (94.7%) by stool antigen testing at 2 months; in those rescoped, biopsy-based RUT at 6 months. Among these, nine patients provided paired gastric biopsy samples at both baseline and six months post-treatment, allowing for a longitudinal assessment of microbial recovery dynamics following eradication.

Across all 121 gastric biopsy samples, the number of unique microbial taxa increased progressively with finer taxonomic resolution—from 7 phyla and 14 classes to 60 genera and 121 species (Fig. 1). This stepwise increase demonstrates the superior discriminatory power of species-level profiling compared with higher taxonomic ranks. Notably, genus-level analysis captured only about half of the distinct taxa resolved at the species level, underscoring the advantage of full-length 16 S rRNA sequencing for precise characterization of the gastric microbiome. To assess within-sample diversity, alpha diversity indices were compared before and after therapy. A marked and statistically significant increase in microbial diversity was observed following eradication. The Shannon index rose from 0.46 ± 0.10 before treatment to 2.17 ± 0.20 after eradication ($p < 0.001$, paired *t*-test), while the Simpson index increased from 0.22 ± 0.07 to 0.81 ± 0.08, reflecting a significant recovery in both richness and evenness (Fig. 5A–B).

These results indicate that *H. pylori* clearance enables recolonization of the gastric niche by a broader set of commensal taxa. Consistent with prior studies, this rebound in diversity supports the concept of a partially reversible dysbiosis following eradication therapy. PCoA based on Bray–Curtis dissimilarity further revealed that post-treatment communities shifted distinctly away from the pre-treatment HP+ cluster and moved toward the HP– group, demonstrating partial ecological restoration of the gastric microbiome (Fig. 5C). To visualize overall taxonomic patterns, relative abundance profiles were examined across infection states. HP+ microbiomes were overwhelmingly dominated by *H. pylori*, which constituted 91.8% ± 3.9% of all bacterial sequences. At higher taxonomic levels, eradication was associated with reduced Helicobacteraceae dominance and increased representation of non-Helicobacter taxa commonly observed in the upper gastrointestinal tract, including members of the Streptococcaceae, Veillonellaceae, and Prevotellaceae families. In contrast, HP– samples contained less than 3% *H. pylori* on average, emphasizing the sharp compositional dichotomy driven by infection status (Fig. 2).

Stacked bar plots (Fig. 2) vividly depict this imbalance: HP+ communities were almost entirely monopolized by *H. pylori*, whereas HP– samples displayed much higher microbial heterogeneity, enriched with oral and commensal genera such as *Streptococcus*, *Prevotella*, and *Veillonella.* This striking difference reflects the ecological collapse induced by *H. pylori* colonization, followed by community diversification once the organism is removed. Importantly, no other Helicobacter species were detected, confirming the species-specific dominance of *H. pylori* within the gastric ecosystem. We next compared diversity metrics between HP + and HP– groups at baseline to quantify the magnitude of dysbiosis.

HP– samples exhibited substantially higher richness and evenness, with a mean Shannon index of 2.08 ± 0.25 and a Simpson index of 0.85 ± 0.07, compared with the severely reduced indices observed in HP+ samples (Fig. 3A–B). To evaluate the biological magnitude of these differences, effect sizes were calculated using Cohen's d.

Table 5 D. Distribution of OLGA and OLGIM stages at baseline

Stage	OLGA *n* (%)	OLGIM *n* (%)
0	82 (75.9%)	76 (70.4%)
I	20 (18.5%)	22 (20.4%)
II	5 (4.6%)	7 (6.5%)
III	1 (0.9%)	2 (1.9%)
IV	0 (0.0%)	1 (0.9%)

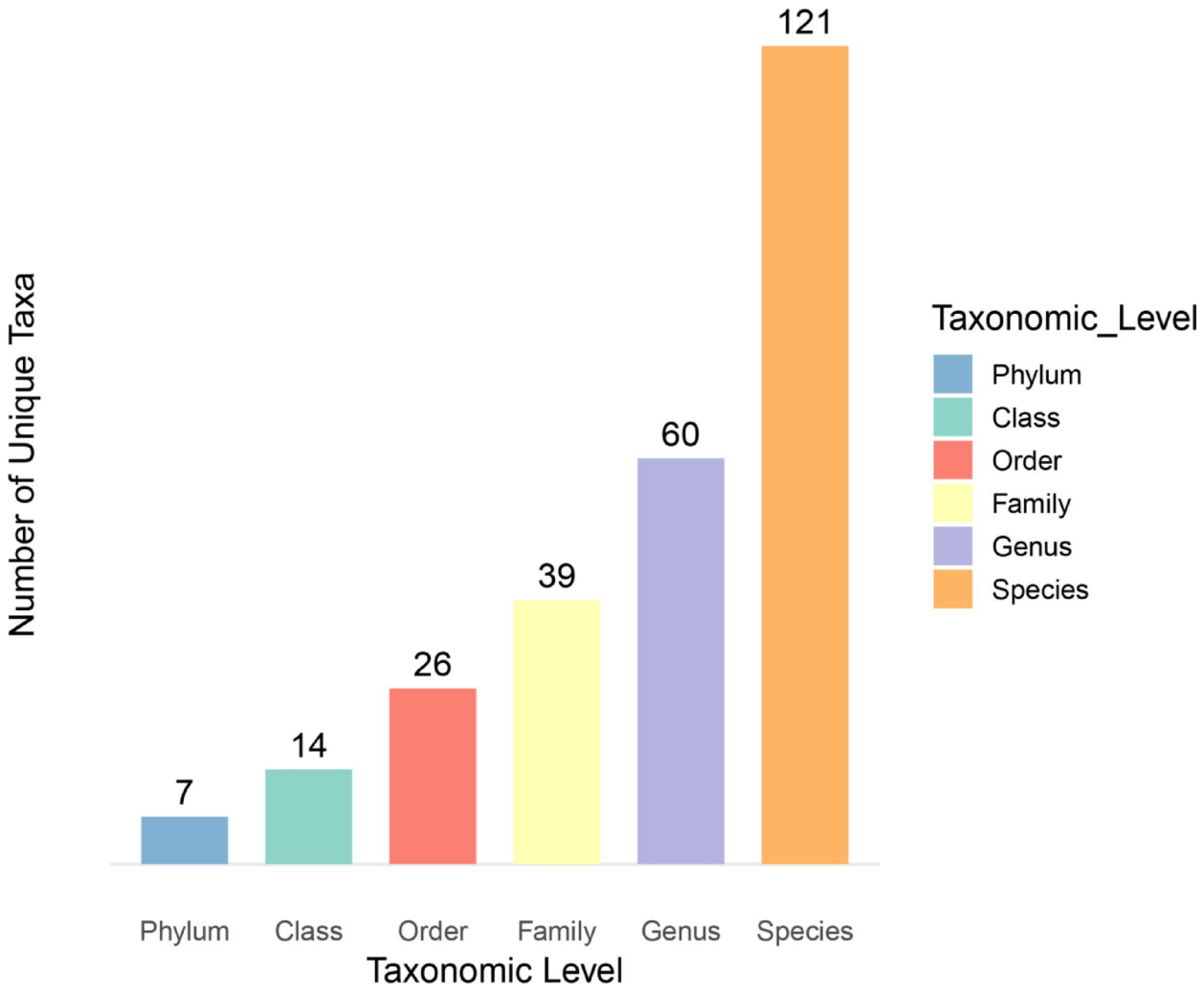

Fig. 1 Microbial diversity across taxonomic levels. Bar plot illustrating the number of unique taxa identified at successive taxonomic ranks (phylum, class, order, family, genus, and species). The number of unique taxa increased progressively with finer resolution, reaching 121 distinct species

The effect size for the Shannon index difference was 1.82, and for the Simpson index, it was 1.76, both indicating significant and biologically meaningful differences. These findings confirm that chronic infection is associated not only with statistically significant but also with functionally considerable loss of microbial diversity. Furthermore, beta diversity analysis based on Bray–Curtis dissimilarity confirmed distinct clustering of HP + and HP– samples (PERMANOVA $R^2 = 0.38$, $p < 0.001$), reinforcing the conclusion that infection status drives major structural rearrangements of the gastric microbiota (Fig. 3C). To identify key taxa contributing to these group differences, indicator species and logistic regression analyses were performed. Multiple commensal organisms—including *Streptococcus mitis*, *Veillonella dispar*, and *Granulicatella adiacens*—were significantly depleted in HP+ samples. Logistic regression yielded odds ratios consistently < 1, indicating that these taxa were negatively associated with infection and suppressed in the presence of *H. pylori* (Fig. 4).

Conversely, HP– samples harbored a more diverse spectrum of low-abundance taxa that collectively contributed to community stability. Heatmap visualization further illustrated the contrast, revealing a greater number of unique species in HP– samples compared with HP+, underscoring the profound ecological simplification characteristic of chronic infection (Fig. 3D). These results demonstrate that chronic *H. pylori* colonization drives near-complete dominance by the pathogen, leading to collapse of microbial diversity and suppression of numerous commensal species.

Histology and endoscopic changes of Pre- and six months Post-Eradication

In the eradication-confirmed group ($n = 54$), paired histological and endoscopic evaluations were available for nine patients at six months post-treatment, enabling a

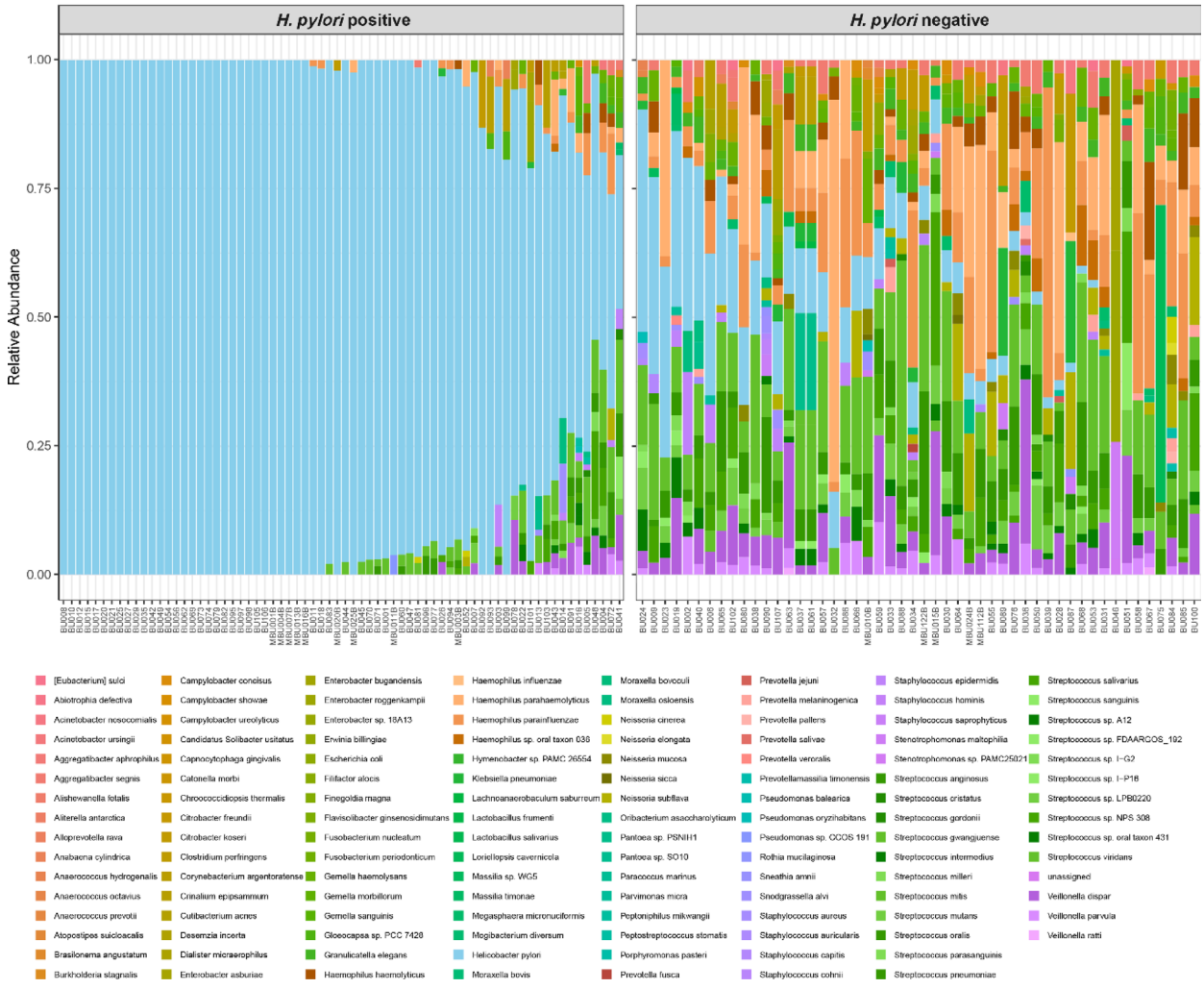

Fig. 2 Relative abundance of gastric microbiota in *Helicobacter pylori*–positive and –negative individuals. Stacked bar plots showing species-level relative abundance profiles stratified by *H. pylori* infection status. In *H. pylori*–positive individuals, the microbiome was overwhelmingly dominated by *H. pylori*, whereas *H. pylori*–negative individuals exhibited markedly greater microbial diversity, with enrichment of commensal taxa such as *Streptococcus*, *Prevotella*, and *Veillonella*

detailed assessment of mucosal healing dynamics. Histological analysis demonstrated marked improvement in chronic active gastritis after *H. pylori* eradication. Both antral and corporal activity scores decreased significantly ($p < 0.05$, Table 5). Neutrophilic infiltration, a hallmark of acute inflammation, had almost completely resolved by six months, indicating suppression of acute inflammatory activity. Mononuclear cell infiltration also declined, reflecting partial recovery of the chronic inflammatory milieu, although levels did not return to those observed in HP– controls. In contrast, premalignant lesions such as intestinal metaplasia and glandular atrophy showed little to no change during the six-month follow-up (Table 6). This stability is consistent with the established understanding that structural mucosal changes reverse only slowly, if at all, despite eradication. These findings highlight the biological distinction between reversible inflammatory activity and relatively fixed atrophic or metaplastic alterations.

Longitudinal histological staging based on the OLGA and OLGIM systems revealed minimal short-term change over the six-month follow-up. Among the nine paired cases, five patients (55.6%) remained at the same OLGA stage, three (33.3%) showed one-stage improvement, and one (11.1%) exhibited no progression but persistent Stage II atrophy. OLGIM staging demonstrated a similar pattern, with seven patients (77.8%) maintaining their baseline stage and two (22.2%) showing minor regression from Stage II to I. No cases showed advancement to higher stages. These results indicate that while active inflammation resolves rapidly after eradication, structural glandular and metaplastic changes progress much more slowly and require longer-term observation (Table 5). Endoscopic assessment corroborated these

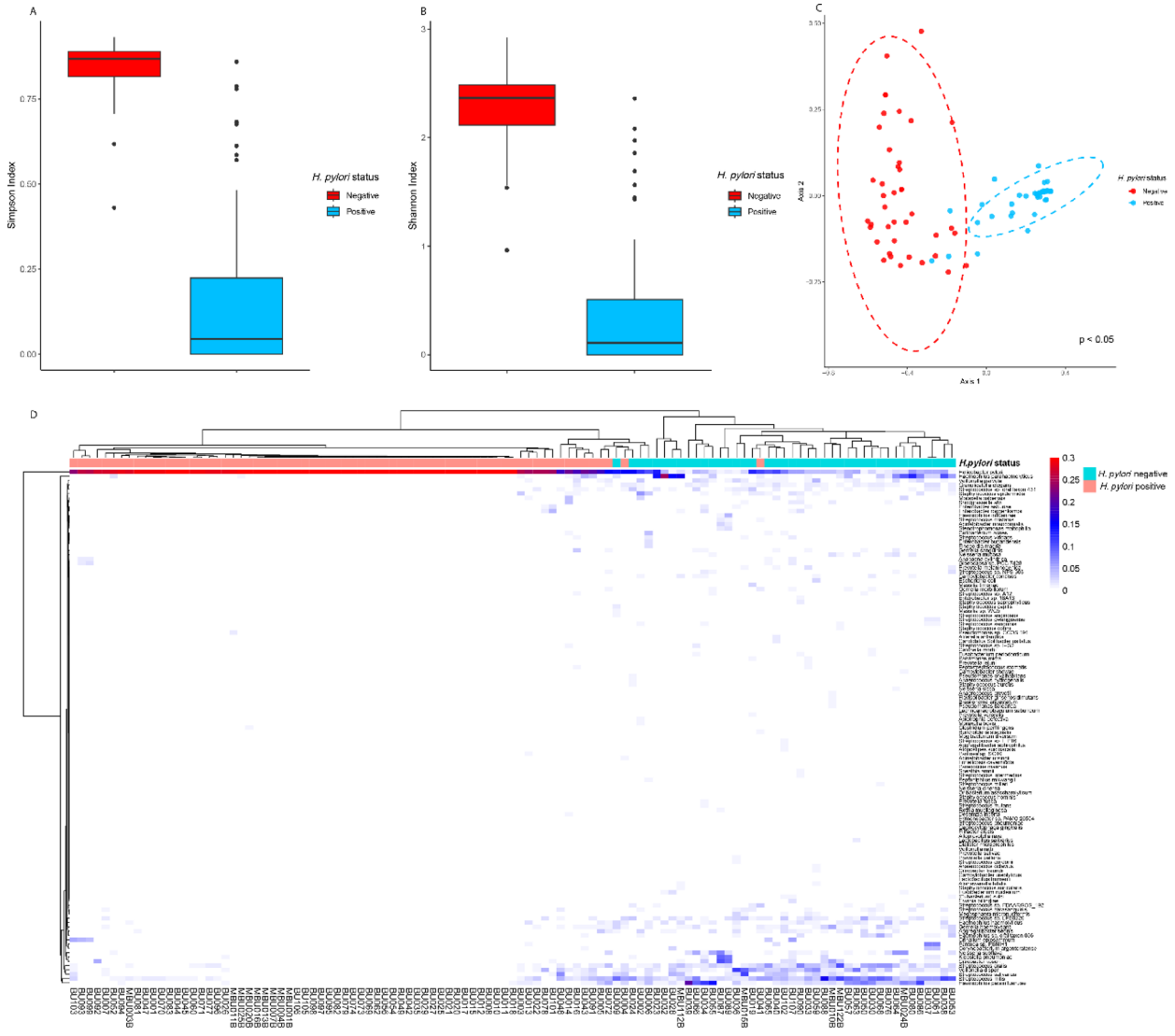

Fig. 3 Diversity indices and community structure of *H. pylori*–positive and –negative gastric microbiota. (**A**) Simpson index and (**B**) Shannon index demonstrating significantly reduced alpha diversity in *H. pylori*–positive compared with negative samples. (**C**) Principal coordinate analysis (PCoA) based on Bray–Curtis dissimilarity showing distinct clustering of the two groups (PERMANOVA, $p < 0.05$). (**D**) Hierarchical clustering heatmap of species-level relative abundance further illustrates the separation of *H. pylori*–positive and –negative microbial communities

trends. The mean Kyoto gastritis score decreased from 4.2 ± 0.7 at baseline to 2.6 ± 0.5 at six months ($p = 0.01$), indicating substantial mucosal improvement. The decline was primarily driven by resolution of diffuse redness and disappearance of nodularity, features strongly associated with active infection. In contrast, components related to atrophy and intestinal metaplasia remained stable, mirroring the histological results. Representative endoscopic images clearly illustrate the post-eradication disappearance of diffuse redness and reduction in mucosal nodularity. These findings demonstrate that *H. pylori* eradication produces rapid and profound resolution of active inflammation. In contrast, premalignant changes such as atrophy and intestinal metaplasia persist beyond short-term follow-up, underscoring the importance of long-term surveillance in high-risk populations.

Microbiome changes Pre- and six months Post-Eradication

Of the 71 HP+ patients, 57 completed quadruple therapy, and eradication was confirmed in 54 (94.7%). This was first determined by stool antigen testing at two months and subsequently by biopsy-based RUT at six months in those who underwent follow-up endoscopy. Among these, nine patients provided paired gastric biopsy samples at baseline and six months post-therapy, enabling exploratory longitudinal microbiome profiling.

To assess within-sample changes, we first examined alpha diversity. Microbial diversity, which was profoundly reduced in HP+ samples at baseline, increased markedly

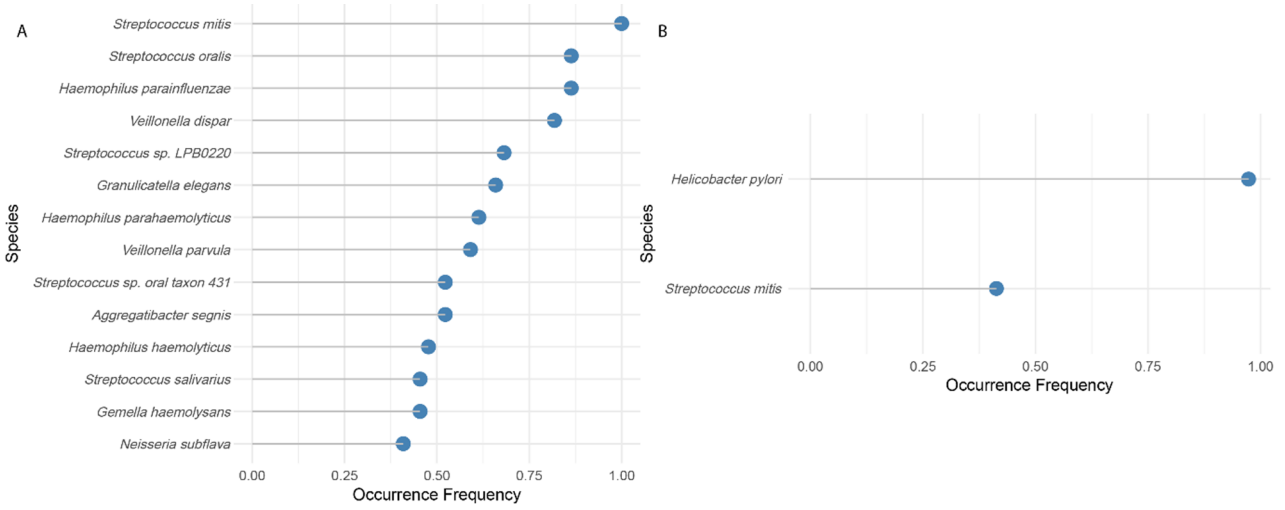

Fig. 4 Core microbiome species occurrence. (**A**) Occurrence frequency of common non-*H. pylori* species across gastric samples, including *Streptococcus mitis*, *Veillonella dispar*, *Haemophilus parainfluenzae*, and *Gemella haemolysans*. (**B**) Comparison of core taxa in *H. pylori*–positive samples, showing the near-universal presence of *H. pylori* together with frequent co-detection of *S. mitis*

Table 6 E. Histological scores before and after *Helicobacter pylori* eradication

Region	Parameter	Pre-treatment (Mean ± SD)	Post-treatment (Mean ± SD)
Antrum	*H. pylori* density	1.33 ± 0.71	0.00 ± 0.00
	Neutrophil infiltration	0.67 ± 0.50	0.11 ± 0.33
	Monocyte infiltration	1.67 ± 0.71	0.78 ± 0.44
	Atrophy	1.22 ± 0.44	1.22 ± 0.44
	Intestinal metaplasia	0.78 ± 0.83	0.78 ± 0.83
Angle	*H. pylori* density	1.33 ± 0.87	0.00 ± 0.00
	Neutrophil infiltration	1.00 ± 0.50	0.44 ± 0.53
	Monocyte infiltration	1.67 ± 0.50	0.67 ± 0.50
	Atrophy	0.78 ± 0.67	0.67 ± 0.50
	Intestinal metaplasia	0.33 ± 0.71	0.56 ± 0.73
Corpus	*H. pylori* density	1.00 ± 0.50	0.00 ± 0.00
	Neutrophil infiltration	1.11 ± 0.78	0.44 ± 0.53
	Monocyte infiltration	1.11 ± 0.60	0.67 ± 0.50
	Atrophy	0.33 ± 0.50	0.33 ± 0.50
	Intestinal metaplasia	0.00 ± 0.00	0.00 ± 0.00

after successful eradication. The Shannon index rose from 0.46 ± 0.10 to 2.17 ± 0.20 ($p < 0.001$, paired *t*-test), and the Simpson index improved from 0.22 ± 0.07 to 0.81 ± 0.08 (Fig. 6A), reflecting broad expansion in both richness and evenness. These findings are consistent with previous reports of post-eradication recovery. Complementary beta diversity analysis using principal coordinate analysis (PCoA) showed that post-treatment at six months, communities shifted distinctly away from the pre-treatment HP+ cluster and toward the HP− group, indicating partial ecological recovery (Fig. 5C). Absolute bacterial quantification further revealed inter-individual variability in post-eradication responses, with consistent reductions in *H. pylori* absolute counts across all paired cases but heterogeneous changes in total bacterial abundance among individuals (Supplementary Figure S1).

Beyond diversity metrics, differential abundance analysis revealed unique taxa enriched in each group (Fig. 6B). HP− controls were enriched with diverse commensals such as *Loriellopsis cavernicola* and *Massilia timonae*, whereas HP+ microbiomes harbored opportunistic organisms, including *Pseudomonas* sp. CC05 19 T and *Paenibacillus* sp. S010, reflecting the perturbed state under chronic infection. Post-eradication samples contained distinct species such as *Herbaspirillum huttiense*, *Stomatobaculum longum*, and *Salmonella enterica*, underscoring that eradication does not restore the microbiome to an uninfected state but instead establishes a novel ecological configuration.

Taxonomic profiling further highlighted recolonization by oral-associated commensals, notably *Streptococcus mitis*, *Neisseria elongata*, and *Prevotella melaninogenica*, consistent with reseeding from the oral cavity. Increases in *Fusobacterium nucleatum* and *Veillonella dispar* were also observed, taxa frequently linked to pro-inflammatory and potentially oncogenic properties [7]. Differential abundance testing identified 174 ASVs that changed significantly after eradication (FDR < 0.05), as visualized in a volcano plot (Fig. 5D). These findings suggest that eradication restores global microbial diversity but does not revert the gastric ecosystem to a pre-infection "normal." Instead, eradication is accompanied by the emergence of new ecological states, including enrichment of taxa with potential pathogenic relevance. This indicates that while eradication reverses *H. pylori*–driven dysbiosis, the long-term clinical implications of the newly established microbiome remain uncertain and warrant continued monitoring.

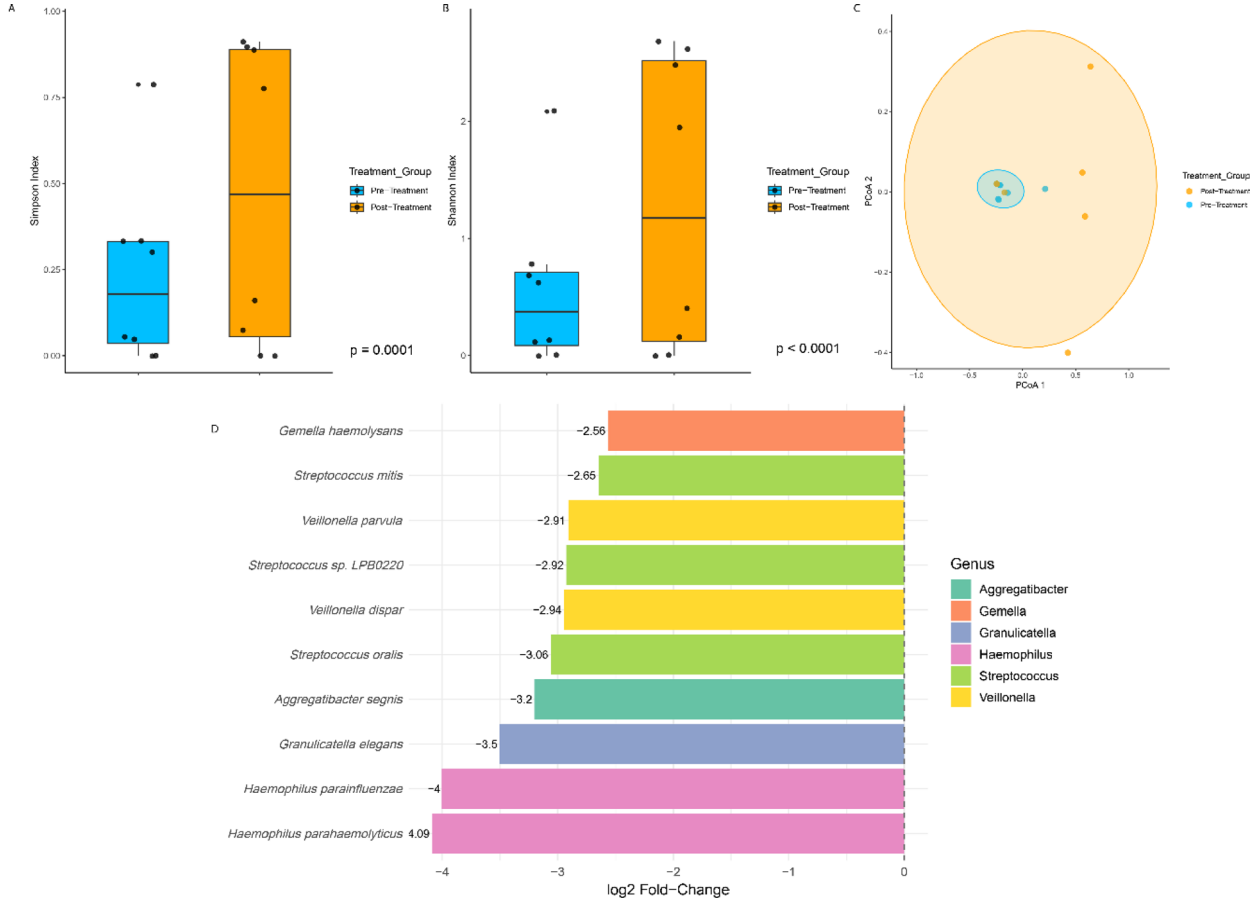

Fig. 5 Microbial diversity and composition pre- and post-***H. pylori*** eradication therapy. (**A**, **B**) Boxplots of Shannon and Simpson indices, respectively, showing significant increases in diversity following eradication therapy ($p < 0.001$). (**C**) PCoA plot displaying distinct community shifts between pre-treatment and post-treatment groups. (**D**) Differential abundance analysis ($\log_2$ fold-change) highlighting post-treatment enrichment of oral-associated taxa including *Streptococcus*, *Veillonella*, *Gemella*, and *Haemophilus* species

Differential abundance analysis (Fig. 5D) revealed enrichment of oral-derived taxa, including *Streptococcus mitis*, *Gemella haemolysans*, *Veillonella dispar*, *Granulicatella elegans*, and *Haemophilus parainfluenzae*, following eradication. These facultative pathobionts have been implicated in persistent mucosal inflammation and early gastrointestinal carcinogenesis. Consistent with this, histological examination demonstrated rapid resolution of neutrophilic activity but persistent mononuclear (monocyte) infiltration six months after therapy, indicating incomplete immunologic normalization. Together, these results suggest that eradication establishes a transitional microbial community that restores diversity yet continues to stimulate low-grade inflammation, paralleling the slow histological recovery of the gastric mucosa [36].

Importantly, these microbial changes paralleled histological and endoscopic improvements. In the eradication-confirmed group, neutrophilic activity resolved, and Kyoto scores declined, while atrophy and intestinal metaplasia remained essentially unchanged. This integrated perspective highlights that eradication drives rapid inflammatory resolution and microbial diversification, whereas structural mucosal changes and complete ecological normalization remain incomplete at six months. Given the limited number of paired samples and the single six-month follow-up timepoint, these longitudinal observations should be interpreted as hypothesis-generating rather than definitive.

Comparison of Post-Eradication and HP− microbiomes

At six months after successful eradication therapy, post-eradication microbiomes exhibited alpha diversity indices that were statistically indistinguishable from those of HP− controls. The Shannon index was 2.17 ± 0.20 in post-eradication samples versus 2.08 ± 0.25 in HP− controls ($p > 0.05$), and the Simpson index was 0.81 ± 0.08 versus 0.85 ± 0.07, respectively (Fig. 6A). These results indicate that eradication rapidly restores within-sample richness and evenness, reversing the profound diversity loss observed in HP+ patients.

Taxonomic composition also showed broad convergence with HP− controls. In both groups, no single

Fig. 6 Comparative mean relative abundance across infection and treatment groups. (**A**) Stacked bar plots of mean relative abundance for *H. pylori*–positive, *H. pylori*–negative, and post-treatment samples. (**B**) Differential abundance analysis identifying group-specific taxa: *Loriellopsis cavernicola* and *Massilia timonae* enriched in *H. pylori*–negative samples; *Pseudomonas* sp. CCO5 19T and *Paenibacillus* sp. S010 enriched in *H. pylori*–positive samples; and *Herbaspirillum huttiense*, *Stomatobaculum longum*, and *Salmonella enterica* enriched in post-treatment samples

genus exceeded 15% relative abundance, and the gastric microbiome was dominated by oral- and commensal-associated genera such as Streptococcus, Prevotella, Veillonella, and Neisseria (Fig. 6A). This balanced structure contrasted sharply with pre-treatment HP+ samples, where *H. pylori* monopolized more than 90% of relative abundance, suppressing nearly all other taxa.

Despite these broad similarities, between-sample comparisons revealed incomplete ecological normalization. Bray–Curtis dissimilarity analysis showed that post-eradication communities remained significantly distinct from HP– controls (PERMANOVA $R^2 = 0.12$, $p = 0.02$), suggesting residual architectural differences at the community level (Fig. 6B).

This partial convergence paralleled the mucosal findings from paired histological and endoscopic examination. While chronic active gastritis scores decreased markedly after therapy and neutrophilic infiltration largely resolved, premalignant features such as intestinal metaplasia and glandular atrophy showed little short-term improvement. Endoscopically, mean Kyoto gastritis scores declined from 4.2 ± 0.7 at baseline to 2.6 ± 0.5 at six months ($p < 0.05$), primarily due to resolution of diffuse redness and nodularity, whereas atrophy- and IM-related components remained largely unchanged.

Unique taxa signatures across infection States

Across the 121 gastric biopsy samples, the number of unique microbial taxa increased progressively with taxonomic resolution, from 7 phyla and 14 classes to 60 genera and 121 species (Fig. 1). This stepwise increase underscores the enhanced discriminatory power of species-level profiling compared with genus-level analysis, which captured only about half of the distinct taxa resolved by full-length 16 S sequencing.

Each clinical state (HP+, HP–, and post-eradication) was associated with a distinct set of unique species (Fig. 6B). HP+ samples contained taxa such as *Pseudomonas* sp. CC05 19 T and *Paenibacillus* sp. S010, which were absent in both HP– and post-eradication groups. HP– controls harbored distinct commensals including *Loriellopsis cavernicola* and *Massilia timonae*. Post-eradication samples formed a third, ecologically distinct cluster, enriched with *Herbaspirillum huttiense* and *Stomatobaculum longum*. These findings indicate that eradication does not simply revert the microbiome from an HP+ state to the HP– baseline, but instead generates a novel ecological configuration defined by unique taxa not observed in either baseline group.

Network analysis

Correlation network analysis highlighted the profound ecological shift following eradication. In pre-treatment HP+ samples, microbial networks were overwhelmingly dominated by *H. pylori*, which acted as a monopolizing hub species. Few other taxa showed meaningful correlations, reflecting the near-complete suppression of microbial interactions under chronic infection. In contrast, post-treatment networks displayed a richer and more interconnected community structure. Taxa such as *Granulicatella elegans*, *Veillonella parvula*, and *Aggregatibacter segnis* emerged as central nodes, suggesting their importance in the early stages of community reassembly. These organisms have previously been associated with oral and upper aerodigestive tract niches, consistent with the reseeding hypothesis of gastric recolonization after eradication. Notably, some abundant commensals, including *Streptococcus mitis* and *Veillonella dispar*, remained at the network periphery. This indicates that while these taxa recolonize the gastric niche rapidly in terms of abundance, they have not yet developed strong ecological interconnections within the broader community. Such incomplete integration suggests that functional restructuring of the gastric microbiome is still ongoing at six months post-eradication. Together, the network analysis illustrates a dynamic, two-phase recovery process: an initial rapid increase in diversity with recolonization by oral commensals, followed by a slower re-establishment of complex ecological relationships. This trajectory parallels the histological findings of rapid resolution of inflammation but persistent atrophy and intestinal metaplasia, underscoring that both microbial and mucosal ecosystems require longer timeframes for full normalization.

Discussion

This study provides one of the first species-level characterizations of gastric microbiome dynamics in a high-risk Mongolian cohort before and after *H. pylori* eradication. Consistent with prior reports [1–3], chronic *H. pylori* colonization induced profound dysbiosis, with near-complete pathogen dominance and marked suppression of commensal taxa. By applying full-length 16 S rRNA sequencing on the Nanopore platform, we resolved over 120 species across gastric samples, providing broader taxonomic coverage than short-read approaches [16]. This higher resolution enabled precise identification of indicator species and detection of group-specific taxa not apparent at the genus level. Importantly, no other *Helicobacter* species were detected, underscoring the specificity of *H. pylori* as the dominant gastric pathogen in this high-incidence population.

By applying full-length 16 S rRNA (V1–V9) sequencing on the Oxford Nanopore platform, this study achieves substantially higher taxonomic resolution than short-read 16 S approaches, which are often unable to distinguish closely related gastric and oral-associated species. Long-read sequencing enables coverage of all variable regions within a single molecule, improving species-level

discrimination in complex polymicrobial samples. Taxonomic assignment was further strengthened using the EMU pipeline, which is specifically optimized for Nanopore full-length 16 S data and has demonstrated superior species-level accuracy compared with conventional classifiers [16]. At six months post-eradication, microbial diversity increased significantly, with Shannon and Simpson indices approaching those of *H. pylori*–negative controls [14]. This rapid rebound was largely driven by oral-derived commensals such as *Streptococcus mitis*, *Neisseria elongata*, and *Prevotella melaninogenica*, consistent with the oral cavity acting as a reservoir for recolonization [37]. Nevertheless, beta diversity analyses demonstrated that post-eradication communities remained significantly distinct from HP– controls, clustering in an intermediate ecological state [14]. These results indicate that eradication initiates—but does not complete—microbial restoration within six months. Consistent with this interpretation, prior longitudinal studies incorporating multiple post-eradication timepoints have demonstrated continued microbial restructuring beyond six months, suggesting that gastric microbiome recovery may extend over 12 months or longer [14, 38]. Given that Mongolian *H. pylori* populations include higher-risk genomic subgroups, strain background may shape post-eradication trajectories and residual risk [8].

Each infection state (HP+, HP–, and post-eradication) was associated with a distinct set of unique taxa, suggesting that eradication generates a novel ecological configuration [38], rather than simply reverting to the HP– baseline. Species-level profiling was critical to revealing these subtle differences, which would have been obscured at higher taxonomic ranks.

Of particular concern is the persistence and enrichment of taxa with oncogenic or pro-inflammatory potential, notably *Fusobacterium nucleatum* and *Veillonella dispar*. *F. nucleatum* has been implicated in both gastric and colorectal carcinogenesis, raising the possibility that its persistence may sustain residual gastric cancer risk even after *H. pylori* clearance [39, 40]. Network analysis further showed that while taxa such as *Granulicatella elegans*, *Veillonella parvula*, and *Aggregatibacter segnis* emerged as central nodes post-eradication, abundant commensals, including *Streptococcus mitis* and *Veillonella dispar*, remained peripheral. This suggests that recolonization is rapid in abundance, but that stable ecological integration is incomplete within six months. Several taxa enriched following eradication—*Streptococcus mitis*, *Gemella haemolysans*, *Veillonella dispar*, *Granulicatella elegans*, and *Haemophilus parainfluenzae* (Fig. 5D)—are oral-derived facultative pathobionts previously linked to persistent gastric inflammation and early gastrointestinal carcinogenesis. Their re-emergence, together with the continued presence of mononuclear infiltration on histology, suggests that ecological and immunologic recovery of the gastric mucosa remains incomplete at six months post-treatment. On the other hand, recent advances in full-length 16 S rRNA sequencing, as used in this study, might enable improved species-level differentiation of oral taxa in gastric microbial community, and a recent study also demonstrated superior taxonomic accuracy for saliva samples using the Emu pipeline [41].

Taxa unique to the post-eradication group, including *Herbaspirillum huttiense*, *Stomatobaculum longum*, *Salmonella enterica*, and *Dialister invisus* (Fig. 6B), support the existence of a transitional dysbiotic state dominated by opportunistic species. This trajectory mirrors the histologic pattern of rapid resolution of active inflammation but persistence of atrophy and intestinal metaplasia, emphasizing that both microbial and mucosal restoration likely require extended periods for full normalization [36]. These findings suggest that eradication therapy alone may not fully re-establish gastric eubiosis within six months and that adjunctive interventions—such as probiotics or prebiotics—should be explored to promote more complete ecological recovery [36]. These shifts may facilitate mucosal healing, although direct functional validation was beyond the scope of this study. Future integration of metagenomics and metabolomics will be essential to confirm these adaptations and to delineate their clinical significance [42].

Several limitations should be noted. The longitudinal cohort was small, with nine paired biopsies at a single six-month follow-up time point; therefore, longitudinal findings should be interpreted as exploratory and may not capture longer-term stabilization of the post-eradication microbiome. In addition, although Nanopore-based full-length 16 S rRNA sequencing provides improved species-level resolution compared with partial 16 S rRNA sequencing based short-read approaches, this platform is characterized by higher per-read error rates, and taxonomic assignment depends on consensus sequence generation and reference database completeness. Consequently, closely related species and low-abundance taxa may remain difficult to resolve with complete certainty. Nonetheless, recent profiling using V3–V4 Illumina sequencing and full-length 16 S rRNA sequencing on ONT platforms showed strong agreement in microbial community composition across different sampling sites within the same organ, such as tracheal aspirates [43]. Moreover, the convergence of findings across diversity metrics, taxonomic profiling, unique taxa signatures, and network analysis in this study supports the robustness of the observed post-eradication community shifts.

Taken together, our results delineate a two-stage ecological trajectory: eradication rapidly restores diversity and suppresses pathogen dominance, but fine-scale taxonomic composition and microbial networks remain

altered. These findings highlight the need for larger-scale, long-term studies in high-incidence populations to determine whether persistent microbial and mucosal alterations influence gastric cancer risk. Further, a longer follow-up (12–24 months) is ongoing in this cohort and will clarify the durability of recovery and its clinical implications. Moreover, adjunctive interventions—such as probiotics, prebiotics, or dietary strategies—should be evaluated as potential means to accelerate ecological normalization and reduce residual malignant potential [44, 45].

Conclusion

This study, to our knowledge, provides the first species-level characterization of the gastric microbiome in a high-risk Mongolian cohort using full-length 16 S rRNA sequencing on the Nanopore platform. Compared with conventional short-read approaches, this method achieves greater taxonomic resolution, underscoring the value of long-read sequencing for accurate gastric microbiome profiling. Our findings demonstrate that the number of taxa detected was substantially higher than in previous studies and that *H. pylori*–positive, *H. pylori*–negative, and post-eradication states exhibited distinct microbial signatures. These results indicate that eradication therapy establishes a new microbial equilibrium rather than fully reverting to the pre-infection community structure. Collectively, the data supports a two-phase model of recovery characterized by an initial rebound in diversity and inflammation resolution, followed by incomplete normalization of microbial and histological networks with persistence of condition-specific taxa. These findings also suggest that supportive strategies, including microbiome-modulating interventions such as probiotics or prebiotics, may help promote more complete ecological recovery after eradication. Long-term longitudinal studies are required to validate these patterns and clarify their implications for gastric atrophy, intestinal metaplasia, and subsequent cancer risk.

Acknowledgements

The authors thank the clinical staff of Bayan-Ölgii Provincial Hospital, UB Songdo Hospital, Department of Gastroenterology and Hepatology of MNUMS, the Mongolia–Japan Hospital of MNUMS, and Oita University for their assistance with patient recruitment, endoscopic procedures, and sample collection. We sincerely thank Bayarnemekh Chultemsuren, Soyolmaa Dondov, and Amarbayasgalan Zagd for their valuable assistance with sample collection and laboratory support. We are also grateful to the laboratory staff and students at Oita University for technical support with sequencing and data analysis. Finally, we sincerely thank all study participants for their invaluable contributions.

Author contributions

(Author Contributions)Conceptualization: N.R., G.B., S.B., Y.Y.Methodology: N.R., T.M., S.BInvestigation (endoscopy, sample collection, sequencing): N.R., G.B., B.L., A.L., Field coordination & patient recruitment: O.K., D.D.Data curation: N.R., S.B., A.K.Formal analysis (microbiome/statistics): N.R., S.B., A.K.Validation (statistical/methodological): T.M., S.B.Resources: G.B., B.L., A.L., O.K., D.D., Y.Y.Visualization (figure preparation): N.R.Writing – original draft: N.R.Writing – review & editing: S.B., T.M., Y.Y.Supervision: T.M., Y.Y.Project administration: N.R., S.B., Y.YFunding acquisition: O.K, Y.Y.All authors read and approved the final manuscript and agree to be accountable for all aspects of the work.

Funding

This study was supported by the Research Center for Global and Local Infectious Diseases, Oita University (Grant No. 2021B13; K.O.); in part by grants from the Japan Agency for Medical Research and Development (AMED) [Adopting Sustainable Partnerships for Innovative Research Ecosystem (ASPIRE), 23836904; Science and Technology Research Partnership for Sustainable Development (SATREPS), 21357105]; and the Japan International Cooperation Agency (JICA) under the SATREPS program (Y.Y.). Additional support was provided by the Thailand Science Research and Innovation Fundamental Fund, the Bualuang ASEAN Chair Professorship at Thammasat University, and the Center of Excellence in Digestive Diseases, Thammasat University, Thailand.
N.R. was supported by the Japanese Government (MEXT) Scholarship Program for 2022.

Data availability

The raw full-length 16S rRNA sequencing reads (Oxford Nanopore) have been deposited in the NCBI Sequence Read Archive (SRA) under BioProject accession PRJNA1046452 and will be publicly available upon publication.

Declarations

Ethics approval and consent to participate

The study was conducted in accordance with the Declaration of Helsinki. The study protocol was approved by the Ethics Committee of the Ministry of Health of Mongolia (N3, 2015), Mongolian National University of Medical Sciences (N13-02/1A, 2013), and the Ethics Committee of Oita University Faculty of Medicine (Yufu, Japan) (Approval No. 1660). All participants were fully informed of the study objectives and procedures, and written informed consent was obtained before enrollment.

Competing interests

The authors declare no competing interests.

Author details

[1]Department of Environmental and Preventive Medicine, Oita University Faculty of Medicine, Yufu, Japan
[2]Department of Gastroenterology and Hepatology, Mongolian National University of Medical Sciences, Ulaanbaatar, Mongolia
[3]Endoscopy Unit, Mongolia-Japan Hospital, Mongolian National University of Medical Sciences, Ulaanbaatar, Mongolia
[4]Department of Gastroenterology and Endoscopy, UB Songdo Hospital, Ulaanbaatar, Mongolia
[5]The Research Center for Global and Local Infectious Diseases (RCGLID), Oita University, Yufu, Japan
[6]Department of Endoscopy, Bayan-Ölgii Province General Hospital, Ölgii, Mongolia
[7]Department of Medicine, Gastroenterology and Hepatology Section, Baylor College of Medicine, Houston, USA

Received: 30 October 2025 / Accepted: 28 January 2026
Published online: 07 February 2026

References

1. Marshall B, Warren JR. Unidentified curved bacilli in the stomach of patients with gastritis and peptic ulceration. Lancet. 1984;323:1311–5. https://doi.org/10.1016/S0140-6736(84)91816-6.
2. Cover TL, Blaser MJ. *Helicobacter pylori* in health and disease. Gastroenterology. 2009;136:1863–73. https://doi.org/10.1053/j.gastro.2009.01.073.
3. Gantuya B, Bolor D, Oyuntsetseg K, Erdene-Ochir Y, Sanduijav R, Davaadorj D, et al. New observations regarding <i />Helicobacter pylori<i /> and gastric cancer in Mongolia. Helicobacter. 2018. https://doi.org/10.1111/hel.12491.
4. Global Cancer Facts & Figs. 2024. 5th ed. Atlanta: American Cancer Society; 2024.

5. Chen Y-C, Malfertheiner P, Yu H-T, Kuo C-L, Chang Y-Y, Meng F-T, et al. Global prevalence of *Helicobacter pylori* infection and incidence of gastric cancer between 1980 and 2022. Gastroenterology. 2024;166:605–19. https://doi.org/10.1053/j.gastro.2023.12.022.
6. Matsuhisa T. Gastric mucosa in Mongolian and Japanese patients with gastric cancer and *Helicobacter pylori* infection. World J Gastroenterol. 2015;21:8408. https://doi.org/10.3748/wjg.v21.i27.8408.
7. Gantuya BE-SHMT, et al. Gastric mucosal microbiota in a Mongolian population with gastric cancer and precursor conditions. Aliment Pharmacol Ther. 2020;51:745–745. https://doi.org/10.1111/apt.15668.
8. Saruuljavkhlan B, Alfaray RI, Oyuntsetseg K, Gantuya B, Khangai A, Renchinsengee N, et al. Study of *Helicobacter pylori* isolated from a high-gastric-cancer-risk population: unveiling the comprehensive analysis of virulence-associated genes including secretion systems, and genome-wide association study. Cancers (Basel). 2023;15:4528. https://doi.org/10.3390/cancers15184528.
9. Nardone G, Compare D. The human gastric microbiota: is it time to rethink the pathogenesis of stomach diseases? United Eur Gastroenterol J. 2015;3:255–60. https://doi.org/10.1177/2050640614566846.
10. Bik EM, Eckburg PB, Gill SR, Nelson KE, Purdom EA, Francois F, et al. Molecular analysis of the bacterial microbiota in the human stomach. Proc Natl Acad Sci USA. 2006;103:732–7. https://doi.org/10.1073/pnas.0506655103.
11. Aviles-Jimenez F, Vazquez-Jimenez F, Medrano-Guzman R, Mantilla A, Torres J. Stomach microbiota composition varies between patients with non-atrophic gastritis and patients with intestinal type of gastric cancer. Sci Rep. 2014;4:4202. https://doi.org/10.1038/srep04202.
12. Eun CS, Kim BK, Han DS, Kim SY, Kim KM, Choi BY, et al. Differences in gastric mucosal microbiota profiling in patients with chronic gastritis, intestinal metaplasia, and gastric cancer using pyrosequencing methods. Helicobacter. 2014;19:407–16. https://doi.org/10.1111/hel.12145.
13. Kim H-N, Kim M-J, Jacobs JP, Yang H-J. Gastric microbiota associated with gastric precancerous lesions in *Helicobacter pylori*-negative patients. Microorganisms. 2025;13:81. https://doi.org/10.3390/microorganisms13010081.
14. Li TH, Qin Y, Sham PC, Lau KS, Chu K-M, Leung WK. Alterations in gastric microbiota after H. pylori eradication and in different histological stages of gastric carcinogenesis. Sci Rep. 2017;7:44935. https://doi.org/10.1038/srep44935.
15. Hanna A, Abbas H, Yassine F, AlBush A, Bilen M. Systematic review of gut microbiota composition, metabolic alterations, and the effects of treatments on PCOS and gut microbiota across human and animal studies. Front Microbiol. 2025. https://doi.org/10.3389/fmicb.2025.1549499.
16. Curry KD, Wang Q, Nute MG, Tyshaieva A, Reeves E, Soriano S, et al. Emu: species-level microbial community profiling of full-length 16S rRNA Oxford Nanopore sequencing data. Nat Methods. 2022;19:845–53. https://doi.org/10.1038/s41592-022-01520-4.
17. Chen X-H, Wang A, Chu A-N, Gong Y-H, Yuan Y. Mucosa-associated microbiota in gastric cancer tissues compared with non-cancer tissues. Front Microbiol. 2019. https://doi.org/10.3389/fmicb.2019.01261.
18. Fuks G, Elgart M, Amir A, Zeisel A, Turnbaugh PJ, Soen Y, et al. Combining 16S rRNA gene variable regions enables high-resolution microbial community profiling. Microbiome. 2018;6:17. https://doi.org/10.1186/s40168-017-0396-x.
19. Tyler AD, Mataseje L, Urfano CJ, Schmidt L, Antonation KS, Mulvey MR, et al. Evaluation of Oxford Nanopore's MinION sequencing device for microbial whole genome sequencing applications. Sci Rep. 2018;8:10931. https://doi.org/10.1038/s41598-018-29334-5.
20. De Coster W, D'Hert S, Schultz DT, Cruts M, Van Broeckhoven C. NanoPack: visualizing and processing long-read sequencing data. Bioinformatics. 2018;34:2666–9. https://doi.org/10.1093/bioinformatics/bty149.
21. Coker OO, Dai Z, Nie Y, Zhao G, Cao L, Nakatsu G, et al. Mucosal microbiome dysbiosis in gastric carcinogenesis. Gut. 2018;67:1024–32. https://doi.org/10.1136/gutjnl-2017-314281.
22. Ferreira RM, Pereira-Marques J, Pinto-Ribeiro I, Costa JL, Carneiro F, Machado JC, et al. Gastric microbial community profiling reveals a dysbiotic cancer-associated microbiota. Gut. 2018;67:226–36. https://doi.org/10.1136/gutjnl-2017-314205.
23. Dixon MF, Genta RM, Yardley JH, Correa P. Classification and grading of gastritis. Am J Surg Pathol. 1996;20:1161–81. https://doi.org/10.1097/00000478-199610000-00001.
24. Costa LCMC, das Graças Carvalho M, La Guárdia Custódio Pereira AC, Teixeira Neto RG, Andrade Figueiredo LC, Barros-Pinheiro M. Diagnostic methods for *Helicobacter pylori*; medical principles and practice. Med Princ Pract. 2024;33:173–84. https://doi.org/10.1159/000538349.
25. Akeel M, Elhafey A, Shehata A, Elmakki E, Aboshouk T, Ageely H, et al. Efficacy of immunohistochemical staining in detecting *Helicobacter pylori* in Saudi patients with minimal and atypical infection. Eur J Histochem. 2021. https://doi.org/10.4081/ejh.2021.3222.
26. Rugge M, Meggio A, Pennelli G, Piscioli F, Giacomelli L, De Pretis G, et al. Gastritis staging in clinical practice: the OLGA staging system. Gut. 2007;56:631–6. https://doi.org/10.1136/gut.2006.106666.
27. Malfertheiner P, Megraud F, Rokkas T, Gisbert JP, Liou J-M, Schulz C, et al. Management of *Helicobacter pylori* infection: the Maastricht VI/Florence consensus report. Gut. 2022;71:1724–62. https://doi.org/10.1136/gutjnl-2022-327745.
28. Quast C, Pruesse E, Yilmaz P, Gerken J, Schweer T, Yarza P, et al. The SILVA ribosomal RNA gene database project: improved data processing and web-based tools. Nucleic Acids Res. 2012;41:D590–6. https://doi.org/10.1093/nar/gks1219.
29. O'Leary NA, Wright MW, Brister JR, Ciufo S, Haddad D, McVeigh R, et al. Reference sequence (RefSeq) database at NCBI: current status, taxonomic expansion, and functional annotation. Nucleic Acids Res. 2016;44:D733–45. https://doi.org/10.1093/nar/gkv1189.
30. McMurdie PJ, Holmes S. phyloseq: An R package for reproducible interactive analysis and graphics of microbiome census data. PLoS One. 2013;8:e61217. https://doi.org/10.1371/journal.pone.0061217.
31. Anderson MJ. A new method for non-parametric multivariate analysis of variance. Austral Ecol. 2001;26:32–46. https://doi.org/10.1046/j.1442-9993.2001.01070.x.
32. Love MI, Huber W, Anders S. Moderated estimation of fold change and dispersion for RNA-seq data with DESeq2. Genome Biol. 2014;15:550. https://doi.org/10.1186/s13059-014-0550-8.
33. Benjamini Y, Hochberg Y. Controlling the false discovery rate: a practical and powerful approach to multiple testing. J R Stat Soc Ser B Stat Methodol. 1995;57:289–300. https://doi.org/10.1111/j.2517-6161.1995.tb02031.x.
34. Csardi G, Nepusz T. The Igraph software package for complex network research. InterJournal Complex Syst. 2006;1695.
35. Sugano K, Tack J, Kuipers EJ, Graham DY, El-Omar EM, Miura S, et al. Kyoto global consensus report on *Helicobacter pylori* gastritis. Gut. 2015;64:1353–67. https://doi.org/10.1136/gutjnl-2015-309252.
36. Taitz JJ, Tan J, Ni D, Potier-Villette C, Grau G, Nanan R, et al. Antibiotic-mediated dysbiosis leads to activation of inflammatory pathways. Front Immunol. 2025. https://doi.org/10.3389/fimmu.2024.1493991.
37. Ahn J, Chen CY, Hayes RB. Oral microbiome and oral and gastrointestinal cancer risk. Cancer Causes Control. 2012;23:399–404. https://doi.org/10.1007/s10552-011-9892-7.
38. Tsuda M, Asaka M, Kato M, Matsushima R, Fujimori K, Akino K, et al. Effect on <Emphasis Type="Italic">Helicobacter pylori</Emphasis> eradication therapy against gastric cancer in Japan. Helicobacter. 2017. https://doi.org/10.1111/hel.12415.
39. Abed J, Emgård JEM, Zamir G, Faroja M, Almogy G, Grenov A, et al. Fap2 mediates Fusobacterium nucleatum colorectal adenocarcinoma enrichment by binding to Tumor-Expressed Gal-GalNAc. Cell Host Microbe. 2016;20:215–25. https://doi.org/10.1016/j.chom.2016.07.006.
40. Yamamura K, Baba Y, Nakagawa S, Mima K, Miyake K, Nakamura K, et al. Human microbiome *Fusobacterium Nucleatum* in esophageal cancer tissue is associated with prognosis. Clin Cancer Res. 2016;22:5574–81. https://doi.org/10.1158/1078-0432.CCR-16-1786.
41. Esberg A, Fries N, Haworth S, Johansson I. Saliva microbiome profiling by full-gene 16S rRNA Oxford Nanopore Technology versus Illumina MiSeq sequencing. NPJ Biofilms Microbiomes. 2024;10:149. https://doi.org/10.1038/s41522-024-00634-1.
42. Cai Y, Luo Y, Dai N, Yang Y, He Y, Chen H, et al. Functional metagenomic and metabolomics analysis of gut dysbiosis induced by hyperoxia. Front Microbiol. 2023. https://doi.org/10.3389/fmicb.2023.1197970.
43. Gupta A, Cooper VS, Zemke AC. Evaluation of V3–V4 and FL-16S rRNA amplicon sequencing approach for microbiota community analysis of tracheostomy aspirates. mSphere. 2025. https://doi.org/10.1128/msphere.00388-25.
44. Tang B, Tang L, Huang C, Tian C, Chen L, He Z, et al. The effect of probiotics supplementation on gut microbiota after Helicobacter pylori eradication: a multicenter randomized controlled trial. Infect Dis Ther. 2021;10:317–33. https://doi.org/10.1007/s40121-020-00372-9.

45. Petkevicius V, Lehr K, Kupcinskas J, Link A. *Fusobacterium nucleatum*: unraveling its potential role in gastric carcinogenesis. World J Gastroenterol. 2024;30:3972–84. https://doi.org/10.3748/wjg.v30.i35.3972.

Publisher's note